JOURNAL OF CATALYSIS 96, 210–221 (1985)

Structural Sensitivity of CO Adsorption and H_2/CO Coadsorption on Ni/SiO_2 Catalysts

D. G. BLACKMOND[1] AND E. I. KO

Department of Chemical Engineering, Carnegie-Mellon University, Pittsburgh, Pennsylvania 15213

Received February 12, 1985; revised June 17, 1985

The surface structure of a series of Ni/SiO_2 catalysts was probed by CO adsorption and H_2/CO coadsorption using quantitative chemisorption measurements and IR spectroscopy. Preparation method, pretreatment conditions, and metal crystallite size were found to affect the nature of the metal surface for crystallites in the range 2.5–9.0 nm. CO was found to adsorb in linear, bridge, and multiple-CO forms on these supported nickel catalysts. Multiple-CO adsorbs on "defect sites" of low coordination, which increase in number as the heterogeneity of the nickel surface increases. On large crystallites exhibiting a large fraction of bridge-CO adsorption, coadsorption of hydrogen aided in probing the types of surface planes present on the crystallites. A high frequency peak in the bridge-CO region was assigned to twofold bridge-CO on Ni(111) while a low-frequency peak was assigned to two- or fourfold bridge-CO on Ni(100) planes. The coadsorption of H_2 also resulted in an increase in the intensity of the peak for CO adsorption on defect sites, possibly due to increased dipole–dipole interactions between linear and subcarbonyl CO species. CO and CO/H_2 adsorption were found to be sensitive probes for both surface smoothness in terms of the presence of defect sites and surface structure in terms of the types of planes exposed.

INTRODUCTION

The adsorption of CO on small supported metal crystallites can be an elegant probe of their surface structure. Ever since the infrared spectroscopic work of Eischens *et al.* (*1, 2*) in which separate IR peaks were assigned to adsorbed CO in linear and bridge forms, there has been a wealth of experimental work involving CO adsorption on a variety of transition metals (*3, 4*). An excellent review of IR spectroscopic studies of CO adsorption on metal catalysts through the mid-1970's was made by Sheppard and Nguyen (*3*). While these studies reveal the rich chemistry of CO adsorption on supported metals, they also show some inconsistencies, including at times large differences between CO spectra from seemingly similar samples. The heterogeneity of supported metal crystallites poses significant problems in attempts to compare differently prepared catalysts. The nature of the metal surfaces is often not sufficiently understood to explain the spectral differences observed in IR studies of CO adsorption.

The objective of this paper is to show that careful IR studies of CO adsorption on supported metal catalysts may be combined with results from other characterization tools and with literature results for well-defined single-crystal surfaces to provide a better understanding of the nature of the metal surface structure of supported crystallites. A series of Ni/SiO_2 catalysts was prepared by different methods and characterized by a battery of chemical and physical techniques (*5*). Infrared spectroscopic studies of CO adsorption and H_2/CO coadsorption were used to probe the surface of the supported nickel crystallites. Combined with results from quantitative H_2 and CO chemisorption measurements, these studies demonstrate how the surface structure of heterogeneous nickel crystallites is related

[1] Present address: Department of Chemical and Petroleum Engineering, University of Pittsburgh, Pittsburgh, Pa. 15261.

0021-9517/85 $3.00

TABLE 1

Catalyst Characterization[a]

Catalyst	Preparation method[b]	wt% Ni	Reduction conditions time (h)/Temp. (K)	% Red[c]
A-30	IW	30	4/773	100
Cl-20	P	20	15/1050	100
A-8	IW	8	4/773	100
A-18	IW	18	4/773	100
C-20	P	20	4/773	70

[a] Data for samples Cl-20, A-8, and C-20 are taken from Ref. (*8*).
[b] IW, incipient wetness impregnation; P, precipitation.
[c] Determined by volumetric O_2 uptake at 673 K.

to catalyst preparation method, metal crystallite size, and pretreatment conditions.

EXPERIMENTAL

The preparation of the Ni/SiO_2 catalysts is described elsewhere (*5*). Briefly, catalysts with a range of crystallite sizes from 2.5 to 9.0 nm were prepared either by incipient wetness impregnation with nickel nitrate hexahydrate or by a precipitation method using a nickel nitrate hexammine solution (*6*). Catalysts were dried in air overnight at 353 K after preparation and were stored in a desiccator until use. Reduction times and temperatures varied for each catalyst, but all were completed in flowing H_2 at 50 cm^3/min after a temperature ramp of 10 K/min to the desired temperature. Reduced samples were evacuated at 10^{-6} Torr and 773 K for 1 h prior to adsorption measurements. Catalyst descriptions, including weight loadings and reduction conditions, are given in Table 1. Metallic weight loadings were confirmed by atomic absorption spectroscopy.

Static chemisorption measurements were made in a conventional glass volumetric apparatus equipped with a precision pressure gauge (Texas Instruments) and a diffusion pumping system capable of 10^{-6} Torr vacuum. H_2 adsorption isotherms were performed at room temperature, taking the total uptake and using a stoichiometry of 1 : 1 for H_{ads} : Ni_s (*7*) for crystallite size determinations. For CO, desorption isotherms were performed at 195 K where little tendency for gaseous carbonyl formation has been found (*8*). A second isotherm was performed after a pumping period of approximately 1 h to remove weakly held CO, and the difference between the two isotherms was taken as the equilibrium adsorbed amount. For both H_2 and CO, the equilibration time for the first point on each isotherm was 15 h, and subsequent points were allowed 1–2 h for equilibration. Isotherms were performed in the pressure range 100–400 Torr.

Infrared spectroscopic measurements were made using a Digilab FTS-15C FTIR spectrometer. A glass gas-handling system capable of achieving a 10^{-6}-Torr vacuum was used for sample pretreatment and adsorption of gases. The quartz IR cell used was a conventional T-shaped cell (*9*) with separate zones for heating and for taking spectra. The sample holder was equipped with a quartz-encased magnet for ease of sample movement between zones. NaCl windows were used. Spectra were collected by coadding 100 scans at a resolution of 8 cm^{-1} and referencing against a spectrum of the freshly reduced Ni/SiO_2 catalyst. Self-supporting sample wafers were prepared by pressing approximately 20 mg of sample under 500 psi ($3.4 \times 10^{+4}$ kPa) to form a disk about 18 mm in diameter. IR spectra of CO adsorption were made after dosing small amounts (<1 Torr) of CO on the catalyst at ambient temperature. Formation of gaseous $Ni(CO)_4$ was not observed at these low pressures.

Crystallite size determinations from X-ray diffraction measurements were made using the line-broadening technique (*10*). A Rigaku D-Max spectrometer with a Mo source allowed crystallite size measurements to about 3 nm. Magnetic measurements were made using a Cahn Magnetic Susceptibility System capable of fields up to 10 kOe (*11*).

TABLE 2

Metal Crystallite Sizes (nm)

Catalyst	H_2 CHEM	XRD	Magnetic
A-30	—	9.0	—
Cl-20	6.0	4.5	4.0
A-8	6.0	6.0	4.5
A-18	5.5	4.5	—
C-20	2.5	<3.0	2.5

RESULTS

The preparation and characterization of the catalysts used in this study (with the exception of sample A-18) was discussed in detail previously (*5*, *8*), and pertinent results are summarized in Tables 1 and 2. As shown in Table 2, both preparation method and reduction conditions affect the crystallite size of the catalysts. By varying preparation method and time and temperature of reduction, catalysts with crystallite sizes ranging from 2.5 to 9.0 nm were prepared.

Table 3 lists chemisorption results (after Ref. (*8*)) from CO and H_2 isotherms for some catalysts. While the $H_{ads}:Ni_s$ ratio has been well established (*7*) to be 1 : 1, the stoichiometry of CO adsorption is more complex since different forms of adsorbed CO with differing stoichiometries may be present on the same catalyst. Study of the ratio of $CO_{ads}:H_{ads}$ may suggest whether bridge or multicentered species ($CO_{ads}:H_{ads} < 1$) are more prominent than linear or multiple-CO species ($CO_{ads}:H_{ads} \geq 1$).

Comparison of $CO_{ads}:H_{ads}$ ratios for the catalysts listed in Table 3 reveals that the ratio decreases as the crystallite size increases. The results also show that crystallite size is not the only factor in determining the $CO_{ads}:H_{ads}$ ratio. While the metal crystallites of both catalysts A-8 and Cl-20 are near 6 nm, their $CO_{ads}:H_{ads}$ ratios differ significantly. Reduction conditions may also play a part, since the Cl-20 catalyst was reduced under more rigorous conditions

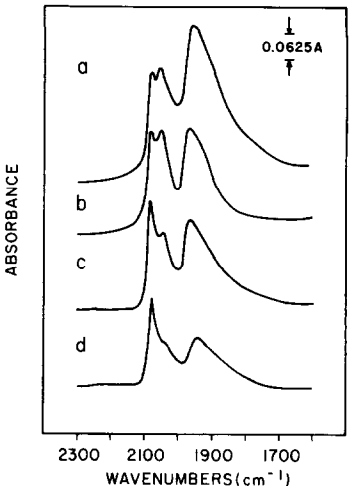

FIG. 1. Spectra of CO adsorption on Ni/SiO_2 catalysts: (a) A-30, (b) Cl-20, (c) A-18, (d) C-20.

than was the A-8 catalyst. A-8 adsorbs nearly twice as much CO per adsorbed hydrogen atom than does Cl-20. This phenomenon is attributed to a larger $CO_{ads}:Ni_s$ stoichiometry on the A-8 catalyst since the results of Table 2 confirm that there is no significant suppression of hydrogen chemisorption on any of the catalysts.

Figure 1 shows IR spectra of CO adsorption at ambient temperature on four reduced Ni/SiO_2 catalysts. Three prominent peaks in the CO stretching region of the IR spectrum are observed for all catalysts. A peak centered near 1950 cm^{-1} was found for all catalysts and is assigned to bridge-CO. The low-frequency side of this peak is

TABLE 3

CO Chemisorption on Ni/SiO_2 Catalysts[a]

Catalyst	Crystallite size[b]/(nm)	$CO_{ads}:H_{ads}$
Cl-20	6.0	0.5
A-8	6.0	0.9
C-20	2.5	1.4

[a] CO chemisorption measured with desorption isotherms at 195 K with an initial dosing pressure of 500 Torr.

[b] As determined by H_2 chemisorption.

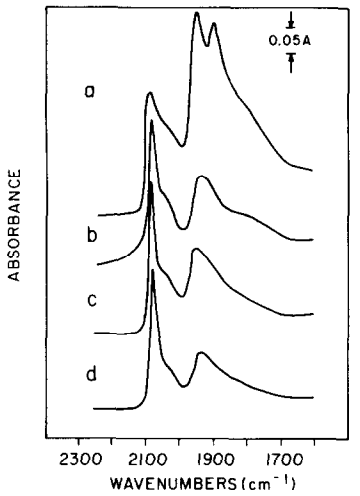

FIG. 2. Spectra of CO adsorption on Ni/SiO_2 catalysts with 100 Torr H_2 added. References are the same as in Fig. 1.

broad and slopes very gradually back to the baseline for all catalysts, suggesting contributions from more than one unresolved peak buried under the broad peak at 1950 cm^{-1}. The spectrum obtained for CO adsorption on A-18 is indentical to that for A-8, which is not shown.

Two peaks of varying relative intensities are found in the linear-CO stretching region for all four catalysts. These peaks are centered at 2040 (LF peak) and 2080 (HF peak) cm^{-1}. As the metal crystallite size increases from 2.5 to 9.0 nm, the relative prominence of the LF peak increases from a small shoulder on the HF peak to a peak of comparable or slighly greater intensity than the HF peak. The relative intensity of the total linear-CO region compared to that of the bridge-CO region also varies with metal crystallite size, becoming less prominent as the crystallite size increases. The HF linear-CO species is weakly held on the surface and may be substantially removed by brief evacuation at ambient temperature. The other peaks are unchanged by this evacuation.

Preparation method and pretreatment as well as metal crystallite size have an effect on the spectra of CO adsorption on this series of catalysts. The spectra of Figs. 1b and c are of catalysts with similar crystallite sizes. However, the relative ratio of the HF/LF peaks is greater for the impregnation catalyst A-18 than it is for the precipitation catalyst Cl-20. As shown in Table 1, Cl-20 was subjected to more rigorous reduction conditions than was A-18. This observation may be compared with that made from the chemisorption results for catalysts A-8 and Cl-20. The impregnation catalyst with the higher CO_{ads} : H_{ads} ratio thus also exhibits a higher HF/LF peak ratio than does the precipitation catalyst of similar crystallite size. While no CO or H_2 chemisorption results are available for catalyst A-30, its IR spectra of CO adsorption and its crystallite size determined by X-ray diffraction support the trends observed for the other catalysts.

When 100 Torr of H_2 was contacted with catalysts with preadsorbed CO, spectra of the CO region as shown in Fig. 2 resulted. One major change in these spectra from those illustrated in Fig. 1 lies in the increase of intensity of the HF linear-CO peak relative to the LF linear-CO peak. This change is present but not quite as pronounced for the 9-nm catalyst A-30 of Fig. 2a. For this catalyst, however, a marked change in the

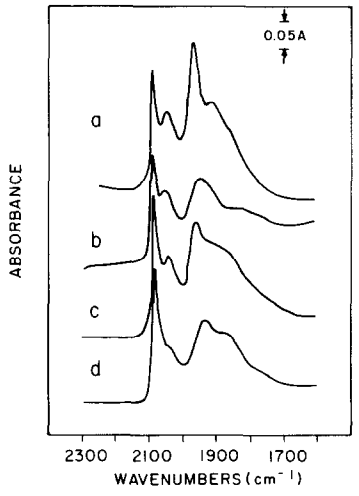

FIG. 3. Spectra of CO adsorption on Ni/SiO_2 catalysts with H_2 preadsorbed. References are the same as in Fig. 1.

bridge-CO region occurs upon addition of H_2 to the CO-covered surface. The broad peak centered near 1950 cm^{-1} shifts down in frequency and separates into two distinct peaks near 1925 and 1880 cm^{-1}.

If, instead of adding H_2 after CO adsorption, H_2 is preadsorbed prior to adsorption of 1 Torr of CO on these catalysts, spectra such as those shown in Fig. 3 are obtained. Prior to CO adsorption, the catalysts were cooled in H_2 following reduction and evacuated briefly at ambient temperature to remove gaseous and weakly held hydrogen, leaving strongly held hydrogen on the surface. In the linear-CO region, the HF peak is again sharp and prominent for all four catalysts. In the bridge-CO region, distinction between separate peaks in the broad absorption band is again most visible for the 9-nm catalyst. The relative importance of the total bridge-CO region with respect to the total linear-CO region increases with crystallite size as for CO adsorption on the bare surface.

DISCUSSION

Both the quantitative chemisorption measurements and the IR spectroscopic studies reveal intriguing differences among the Ni/SiO_2 catalysts employed in this study. The results suggest that preparation method, metal crystallite size, and pretreatment procedures play a significant role in determining the surface structure of supported nickel crystallites.

Chemisorption Results

Chemisorption results revealed CO_{ads}/H_{ads} ranging from 0.5 to 1.4 for different catalysts. In the absence of gaseous nickel carbonyl formation, CO_{ads}/H_{ads} ratios greater than 1 imply the adsorption of more than one CO molecule on a single Ni surface atom. These results were discussed previously (*8*). These multiple-CO species were assigned to subcarbonyl adsorption on "defect" sites. It was found that preparation method, pretreatment, and crystallite size influenced the stoichiometry of CO adsorption on these catalysts. For a given crystallite size of nearly 6 nm, the sample prepared by precipitation and reduced under rigorous conditions (Cl-20) exhibited less subcarbonyl adsorption than did catalysts with similar crystallite sizes prepared by impregnation. It was suggested that the high-temperature reduction treatment required to sinter the precipitation catalyst Cl-20 to nearly 6 nm caused a "smoothing" or annealing of the nickel surface that eliminated "defect" sites necessary for adsorption of multiple CO molecules. Hence subcarbonyl adsorption was attributed not only to low-coordination nickel atoms found on small crystallites as an intrinsic characteristic of their size, but also to highly uncoordinated "defect" sites which can be found on heterogeneous crystallites which have not undergone a surface smoothing treatment.

IR Spectroscopy of CO Adsorption

The IR spectra of CO adsorption on bare nickel surfaces show interesting trends both for crystallite size and for preparation method. While the peak for bridge-CO at 1950 cm^{-1} does not appear to change significantly in shape with these variables, the two peaks in the linear-CO region are influenced, as is the overall ratio of linear/bridge intensity, by both crystallite size and method of preparation. The IR peak at 1950 cm^{-1} representing bridge-CO is broad for all catalysts. This peak is probably the combination of two or more unresolved peaks.

One possibility to explain the broad bridge-CO peak is that CO may be adsorbed on different crystal planes, and on each plane there are different bridging configurations. The frequency of two-fold bridge-CO should increase from Ni(100) to Ni(111) since Ni atoms in the higher density Ni(111) plane have fewer *d*-electrons available for backbonding than do the more uncoordinated nickel sites in (100) and other crystal planes (*3*). However, (111) planes afford the possibility of bridging CO in three-fold sites which would lead to lower frequencies

than are found for twofold bridge-CO on either plane. In addition, a fourfold site for bridge-CO found on (100) planes would provide still lower frequencies (*3*). Examination of the spectra in this light leads to the suggestion that the broad bridge-CO peak for all four catalysts is due mainly to twofold bridge-CO sites with smaller amounts of three- and fourfold bridge-CO sites comprising the asymmetric low-frequency side of the peak.

The ratio of the intensities of the bridge-CO region to the linear-CO region increases with crystallite size. As the small crystallites grow in size, they may form metal surfaces with more long-range order, capable of providing more sites for bridge-CO adsorption.

In the linear-CO region, two peaks appear which vary in relative intensity with particle size and preparation method, as already mentioned. The LF peak at 2040 cm^{-1} has been attributed, in accordance with results for CO adsorption on single-crystal nickel planes (*12–15*), to linear-CO adsorption on planar sites typical of (100) or (110) planes. The assignment of the HF peak near 2080 cm^{-1} is less straightforward.

An IR peak near 2080 cm^{-1} has been observed in previous studies of CO adsorption on nickel. Yates and Garland (*16*) and Garland *et al.* (*17*) attributed the peak to CO weakly adsorbed on "amorphous" nickel, meaning sites with highly disordered structure and incomplete nearest-neighbor coordination. Rochester and Terrell (*18*) also found that the CO species assigned to HF linear peak was weakly adsorbed, but their studies of sulfur poisoning of nickel surfaces led them to suggest the peak is due to multiple coordination of CO on a single nickel atom to form a subcarbonyl species. Bouwman and Freriks (*19*) and Heal *et al.* (*20*) have also suggested that a HF peak of this type be assigned to a subcarbonyl surface species. Primet *et al.* (*21*) suggested that the weakly held HF linear-CO peak could be attributed to CO adsorbed on nickel atoms in contact with unreduced nickel residues, with the electronegative character of the oxide phase withdrawing electrons from the M–CO linkage and hence weakening the adsorption and shifting the IR frequency upward. Comparison of the IR spectra in Fig. 1 with CO_{ads}/H_{ads} ratios from chemisorption measurements in Table 3 reveals that the HF linear-CO peak increases as the CO_{ads}/H_{ads} ratio increases. This suggests that the HF linear-CO peak be assigned to a subcarbonyl species, in agreement with the results of Rochester and Terrell (*18*). Hence, the IR results for CO adsorption support CO chemisorption measurements which indicate that increased subcaronyl adsorption occurs as the nickel crystallite size decreases.

The catalysts whose IR spectra are shown in Figs. 1b and c have similar crystallite sizes and yet the HF/LF ratio is greater for the impregnation catalyst A-18 than for the precipitation Cl-20 catalyst. Again, this trend parallels that found for CO_{ads}/H_{ads} ratios for Cl-20 and A-8 in Table 3, with the greater CO_{ads}/H_{ads} ratio observed for the impregnation catalyst. The IR results therefore support the suggestion that the number of "defect sites" on which the subcarbonyl species forms is smaller on the 6-nm precipitation catalyst, which had undergone the rigorous reduction treatment and smoothing of the surface of the metal crystallites.

The nature of the "defect sites" for subcarbonyl adsorption is not well defined. Multiple CO molecules are weakly adsorbed on these highly uncoordinated sites. The defect sites appear to be due to the disordered structure of heterogeneous metal crystallites and could possibly be found at the junctions between surface planes, which should be greater in number than is expected for crystallites exhibiting ideal geometries.

The 9-nm catalyst A-30 whose spectrum is shown in Fig. 1a exhibits a HF/LF linear-CO ratio slightly smaller than that of the 6-nm catalysts Cl-20, even though A-30 received a less rigorous reduction or

surface-smoothing treatment. The spectra of Fig. 1 also reveal that the bridge-CO peak for A-30 is a much more dominant feature of the CO spectrum than is the bridge-CO peak for Cl-20. The significantly larger size of the crystallite of A-30 produced by impregnation suggests that these crystallites have more extended smooth planes than are found either on impregnation catalysts of smaller crystallite size or on the surfaces of rigorously reduced precipitation catalysts.

These infrared and chemisorption studies support suggestions made in other studies (*18, 22*) that subcarbonyl adsorption decreases with increasing crystallite size. The results reported here suggest further that this trend should more specifically be attributed to increasing surface smoothness rather than simply increasing crystallite size.

Application of group theory (*23*) to spectroscopic studies of molecules adsorbed on surfaces indicates that a dicarbonyl species adsorbed on a single metal atom ought to have two infrared-active vibrations, a high-frequency symmetric and a lower frequency asymmetric vibration. Spectra of this type were found by Yates and co-workers (*24, 25*) for multiple-CO rhodium(I) species. However, the present results for nickel catalysts indicate that only the 2080-cm^{-1} peak is involved in subcarbonyl formation, since changes in this peak after various treatments are not accompanied by parallel changes in any other peaks for adsorbed CO.

It may be possible to explain the absence of the asymmetric component of the subcarbonyl vibration by calling on an infrared "metal-surface selection rule" described by Pearce and Sheppard (*26*). If a dipole such as a CO molecule is situated above the surface of a conducting medium such as a reduced metal crystallite, it will produce a virtual-image dipole in the metal surface. The dipole change for the parallel vibrating molecule is cancelled by the image dipole change, while the dipole changes for the molecule and its image dipole reinforce each other in the perpendicular case. Hence, only dipole changes perpendicular to the surface of a perfect conductor should be infrared active. For the case of a dicarbonyl species absorbed on a reduced metal surface, the lower frequency asymmetric vibration will be infrared inactive as long as the twofold axis of the species is perpendicular to the metal surface.

This metal-surface selection rule may be expected to hold rigorously only in cases where the metal surface may be considered perfectly conducting, or perfectly polarizable. If the surface atoms are oxidized or if the crystallite size becomes very small, then the complete cancellation of parallel dipole/image dipole contributions may not be expected. Metal crystallites in the size range 2.5–9 nm such as those studied here would be expected to follow this selection rule. The absence of an asymmetric stretching CO vibration cannot in itself rule out the existence of an adsorbed subcarbonyl on these nickel surfaces.

As mentioned before, Primet *et al.* (*21*) suggested from their infrared results of CO adsorption on similar Ni/SiO_2 catalysts that the HF linear-CO peak was due to CO adsorbed on nickel in intimate contact with unreduced nickel oxide residues. The catalysts whose spectra are shown in Fig. 1 all exhibited 100% reduction to the metal except for the catalyst C-20 whose spectrum is shown in Fig. 1d, which was 70% reduced. This catalyst also exhibits the largest relative intensity of the HF linear CO peak, and yields a CO_{ads}/H_{ads} ratio greater than 1 from chemisorption measurements. This implies some carbonyl formation on the C-20 catalyst surface. But if this adsorption occurs on partially reduced nickel, the "perfect conductor" requirement for the surface-metal selection rule (*26*) is no longer met, and the out-of-phase asymmetric vibration of the subcarbonyl should become infrared-active. This lower frequency vibration is not observed, suggesting that the unreduced portion of the nickel surface

does not affect the CO adsorption significantly. In fact, the unreduced portion may consist of a hydrosilicate "glue" layer between the support and the nickel, as has been suggested previously (*5, 27, 28*), and hence does not affect the oxidation state of the metal crystallites.

IR Spectroscopy of H_2/CO Coadsorption

Hydrogen has a striking influence on CO adsorption on nickel catalysts for both the different preparation methods and the different crystallite sizes investigated. One important feature is the increase in intensity of the 2080-cm^{-1} HF linear-CO peak compared to the rest of the CO spectrum. This effect is noted for all catalysts, although in differing degrees for different crystallite sizes. The bridge-CO species may also be altered by the presence of hydrogen. The broad bridge-CO band splits into two fairly well-separated bands in the spectrum of CO adsorbed on the catalyst with the largest crystallite size, the 9-nm A-30.

Significantly fewer investigations have been made of the coadsorption of CO and H_2 on metal surfaces than have been made of CO adsorption alone. In infrared studies of Ni/SiO_2 and Ni/Al_2O_3 catalysts, increases in HF linear-CO intensity similar to that observed in the present study were found by Primet and Sheppard (*29*) and by Galuzska and Amenomiya (*30*). A similar HF peak in the CO spectrum for adsorption of CO on Ni/SiO_2 in the absence of H_2 was previously explained (*21*) by suggesting interaction of nickel with oxide residues, as discussed earlier in this paper. This led Primet and Sheppard (*26*) to suggest that the upward shift in CO frequency in the presence of H_2 was due to the electron-attracting power of adsorbed H_2, which causes a shift of metal *d*-electrons to adsorbed hydrogen and hence weakens the metal–CO bond.

Another perspective concerning the origin of the HF linear-CO peak and its behavior in the presence of hydrogen may be obtained from the vibrational spectroscopic results for CO adsorption on single crystals of copper by Hollins *et al.* (*31*). They attributed an unusual high-frequency peak in the linear-CO region to adsorption on defect sites of low metal coordination on a slightly misoriented Cu(110) crystal. They also asserted from isotopic dilution studies that the intensity of the HF linear-CO peak was enhanced significantly above its true value due to strong dipole–dipole coupling effects between CO on defect and planar sites. In fact, a large fraction of the absorbance of the HF linear-CO peak was accounted for in terms of these dipole interactions. It was shown that a very small number of defect sites were responsible for large coupling-induced intensity increases in the HF linear-CO peak. Dipole–dipole interactions of this type have been discussed before, manifested as changes in relative intensities and frequencies of IR peaks with surface coverage or concentration of one isotope (*32, 33*).

Interpretation of the present infrared results for CO adsorption in terms of these suggestions implies that at least part of the intensity of the HF linear-CO is due to strong dipole–dipole interaction between multiply adsorbed CO molecules on the defect sites and linear CO molecules on planar sites, even in the absence of H_2. This effect is greatly enhanced in the presence of hydrogen. Apparently hydrogen may adsorb in such a fashion as to increase coupling between CO on planar and defect sites. This may occur by crowding of the planar CO species into different binding configurations so that they become closer to the plane junctions where the defect sites are most probably located. The number of CO molecules involved in a coupling interaction of this sort may be quite small and still promote the significant intensity increase that was observed here for the HF linear-CO in the presence of hydrogen. The degree of the coupling interaction increases with the heterogeneity of the crystallites and the fraction of defect sites present.

The effect that hydrogen has on the

bridge-CO region of the spectrum for A-30 may suggest that the large crystallites are comprised of extended crystal planes of different types, and that H_2/CO interactions are different on each plane. Comparison of these coadsorption results with those from studies of single crystal surfaces may provide a way to distinguish between the different crystal planes found on the heterogeneous surfaces of the supported nickel crystallites. Some pertinent conclusions drawn from single-crystal results of CO and CO/H_2 adsorption are outlined in the following paragraphs. These conclusions have led us to assign the HF bridge-CO peak at 1925 cm^{-1} in Figs. 2a and 3a to CO adsorbed on Ni(111) planes and the LF bridge-CO peak at 1880 cm^{-1} to CO adsorbed on Ni(100) planes.

The nature of CO adsorption has been found to differ on Ni(100) and Ni(111) surfaces (*12–15, 34, 35*). On Ni(111), the CO stretching frequency was found to increase with coverage in a nonlinear fashion, indicating a change in CO adsorption sites from threefold to twofold as θ increased (*34, 35*). A parallel decrease in the adsorption energy (*35*) led to the conclusion that the major cause of the frequency shift was due to changes in the degree of backdonation of electrons into the $2\pi^*$ antibonding orbitals of CO. On Ni(100), vibrational spectra of adsorbed CO appear to be more complex. The adsorption energy for CO was found to remain relatively constant with increasing coverage (*12*) and was higher than that observed on Ni(111). This implies a lower vibrational frequency for CO on Ni(100) than on Ni(111) when in fact experimental results (*14*) show the opposite for the bridge-CO region. Doyen and Ertl (*36*) have shown theoretically that E_{ad} should reflect primarily the extent of backbonding; hence, the anomalous vibrational frequency sequence $\nu_{CO}(100) > \nu_{CO}(111)$ must be explained in terms of other factors. One such factor may be differences in the importance of CO dipole–dipole interactions for each crystal face. The high frequency for CO found on Ni(100) may be due to a greater interaction between CO dipoles on this crystal face.

These ideas are supported very well by CO/H_2 coadsorption studies by White and coworkers (*37, 38*) which help to complete our picture for the surface structure of the A-30 catalyst. White and co-workers (*37, 38*) found differences in the coadsorption of CO and H_2 on Ni(100) and Ni(111) single crystals. It was suggested from these and other results (*39*) that intimate mixing occurs in the coadsorption on Ni(100) surfaces while on Ni(111) separate islands of CO and H_2 exist on the surface. Adsorption of CO/H_2 at low temperatures (where coverage is likely to be comparable to that achieved in our higher pressure studies of supported Ni) revealed no shift in the bridge-CO peak for Ni(111) in the presence of H_2, while the main bridge-CO peak on Ni(100) shifted from 1955 to 1885 cm^{-1} in the presence of H_2. This frequency shift agrees well with our results for the LF bridge-CO peak of A-30 in the presence of hydrogen. These results taken together suggest that this shift may be due to the relaxation of lateral dipole interactions between CO molecules by the intimately mixed adsorbed hydrogen.

To summarize the findings of these studies of CO and CO/H_2 adsorption on single crystal surfaces, it appears that the frequency of bridge-CO on Ni(111) is relatively unaffected by H_2, while bridge-CO species on Ni(100) exhibit a large downshift in frequency under these conditions, causing the relative frequencies to change to $\nu_{CO}(111) > \nu_{CO}(100)$ as predicted by measurements of energy of desorption (*35*). The frequency of CO adsorption on Ni(100) planes appears to be quite sensitive to the extent of dipole–dipole interactions between CO molecules which can be greatly influenced by the presence of hydrogen intimately mixed with CO. For these reasons we have assigned the HF bridge-CO peak at 1925 cm^{-1} for catalyst A-30 in Figs. 2 and 3 to bridge-CO (twofold) on Ni(111) planes

and the LF bridge-CO peak at 1880 cm^{-1} to bridge-CO (possible a mixture of two- and fourfold) on Ni(100) surfaces. A small amount of threefold bridge-CO on Ni(111) might be indicated by the low-frequency tail of the bridge-CO peak, but probably does not make a significant contribution at the high CO coverages likely under the conditions of these adsorption experiments.

Hence, the peak shift and separation which occurs in the IR spectrum of CO in the presence of hydrogen on A-30 may be attributed to differences in the way bridge-CO species on different crystal planes respond to H_2/CO coadsorption. The significantly larger fraction of bridge-CO species on catalyst A-30 compared to the other catalysts may explain why this effect is pronounced mainly for this catalyst in the series. A-30 may possess a higher degree of extended planes for bridge-CO adsorption, a condition necessary for observation of the effect of hydrogen on these species. H_2/CO coadsorption studies employing increasing amounts of ^{13}CO would be very useful in exploring the effect of hydrogen coadsorption by helping to probe which peaks (and hence, which crystal planes) are more strongly influenced by dipole–dipole interactions (*33, 40*).

The high-frequency bridge-CO peak for the large crystallite size A-30 catalyst is much more dominant than is the rest of the bridge-CO region in the IR spectrum of CO in the presence of hydrogen on this catalyst. The assignment of this peak to adsorption on Ni(111) planes supports reaction results (*41*) suggesting a relationship between increased crystallite size and increased proportion of Ni(111) planes on supported nickel crystallites. Indeed, comparison of CO/H_2 reaction results from our laboratory (*42*) on catalysts A-30 and the small particle size C-20 show significantly higher selectivity to C_2^+ hydrocarbons for A-30.

Several recent studies on supported Pd systems have also used CO adsorption as a probe of the surface structure of the metal crystallites (*43–46*). Results from Pd single-crystal studies were called upon by Hicks *et al.* (*43, 44*) and to characterize CO peaks in the bridge-CO region according to the fraction of Pd(100) and Pd(111) planes present on supported crystallites. Palazov *et al.* (*46*) suggested that changes in the IR spectra of CO adsorbed on Pd/Al_2O_3 after various treatments were due to reconstruction of the Pd surface in the presence of H_2. These studies along with our own results illustrate the use of careful adsorption studies as a promising tool for achieving a better understanding of the surface structure of supported metal crystallites.

CONCLUSIONS

Quantitative chemisorption measurements and IR spectroscopic studies have been used to probe the surface structure of a series of Ni/SiO_2 catalysts with crystallite sizes in the range 2.5–9.0 nm. Preparation method, reduction treatment, and crystallite size were all found to affect the nature of CO adsorption on these catalysts.

CO adsorbs on nickel crystallites in bridge form and linear (LF) form on surface planes, and in multiple-CO (HF) form on defect sites. The defect sites are most probably found at the junctions between truncated surface planes on these many-faceted, heterogeneous crystallites. The relative intensity of the HF subcarbonyl peak in the IR spectrum of CO adsorption depends on the degree of surface heterogeneity, and may also be augmented by dipole–dipole coupling interactions with the planar LF linear-CO species. Coadsorbed H_2 has the effect of increasing these interactions, possibly by pushing linear-CO species into closer proximity to the defect-site CO.

The effect of the addition of hydrogen on CO adsorption was suggested to depend on the type of plane exposed on the crystallite surface. On very large crystallites, whose CO spectra exhibit a large bridge/linear CO intensity ratio, H_2/CO interactions are manifested as a split and shift of the bridge-CO

peak. The HF bridge-CO peak is assigned to twofold bridge-CO on Ni(111) while the downshifted LF bridge-CO peak may be due to two- or fourfold bridge-CO on Ni(100) planes.

These results illustrate how the surface structure of small supported nickel crystallites may be probed by studying CO adsorption and H_2/CO coadsorption on the metal surfaces. As a general conclusion, it appears that CO peaks above 2000 cm^{-1} on supported nickel act as a sensitive probe of the degree of surface smoothness, that is, of the presence of defect sites. The CO region below 2000 cm^{-1} can be a probe for the type of crystal plane exposed if the crystallites are large enough to have extensive smooth planes. This study helps to increase the sophistication of our understanding of the nature of these heterogeneous Ni/SiO_2 catalysts. It is hoped that this development of a better picture of the surface structure of supported nickel crystallites may ultimately enable predictions about their catalytic behavior to be made on a more scientific basis.

ACKNOWLEDGMENTS

The authors would like to acknowledge support for this work from the National Science Foundation (CPE 81-15575), Sun Oil Company Equipment Grant, National Science Foundation Fellowship (D.G.B.), and Union Carbide Supplemental Fellowship (D.G.B.).

REFERENCES

1. Eischens, R. P., Francis, S. A., and Pliskin, W. A., *J. Phys. Chem.* **60,** 194 (1956).
2. Eischens, R. P., and Pliskin, W. A., "Advances in Catalysis," Vol. 10, p. 1. Academic Press, New York, 1958.
3. Sheppard, N., and Nguyen, T. T., *in* "Advances in Infrared and Raman Spectroscopy" (R. J. Clarke and R. E. Hester, Eds.), Vol. 4, p. 67. Wiley, New York, 1978.
4. Yates, J. T., Jr., Madey, T. E., and Campuzano, J. C., "The Physics and Chemistry of Solid Surfaces and Heterogeneous Catalysis" (D. A. King and D. P. Woodruff, Eds.), in press.
5. Blackmond, D. G., and Ko, E. I., *Appl. Catal.* **13,** 49 (1984).
6. Martin, G.-A., Mirodatos, G., and Praliaud, H. A., *Appl. Catal.* **1,** 367 (1981).
7. Bartholomew, C. H., and Pannell, R. B., *J. Catal.* **65,** 390 (1980).
8. Blackmond, D. G., and Ko, E. I., *J. Catal.* **94,** 343 (1985).
9. Ward, J. W., *J. Catal.* **9,** 25 (1967).
10. Klug, H. P., and Alexander, L. E., "X-Ray Diffraction of Amorphous Materials." Wiley, New York, 1974.
11. Selwood, P. W., "Chemisorption and Magnetization." Academic Press, New York/London, 1975.
12. Tracy, J. C., *J. Chem. Phys.* **56,** 2736 (1972).
13. Andersson, S., *Solid State Commun.* **21,** 75 (1977).
14. Bertolini, J. C., Dalmai-Imelik, G., and Rousseau, J., *Surf. Sci.* **68,** 539 (1977).
15. Bertolini, J. C., and Tardy, G., *Surf. Sci.* **102,** 131 (1981).
16. Yates, J. T., Jr., and Garland, C. W., *J. Phys. Chem.* **65,** 617 (1961).
17. Garland, C. W., Lord, R. C., and Troiano, P. F., *J. Phys. Chem.* **69,** 1195 (1965).
18. Rochester, C. W., and Terrell, R. J., *J. Chem. Soc. Faraday Trans. 1* **73,** 609 (1977).
19. Bouwman, R., and Freriks, I. L. C., *Appl. Surf. Sci.* **4,** 21 (1980).
20. Heal, M. J., Leisegang, E. C., and Torrington, R. G., *J. Catal.* **42,** 10 (1976).
21. Primet, M., Dalmon, J. A., and Martin, G. A., *J. Catal.* **46,** 25 (1977).
22. van Hardeveld, R., and Hartog, F., "Advances in Catalysis," Vol. 22, p. 75. Academic Press, New York, 1972.
23. Braterman, P. S., "Metal Carbonyl Spectra." Academic Press, New York/London, 1975.
24. Cavanagh, R. R., and Yates, J. T., Jr., *J. Chem. Phys.* **74,** 4150 (1981).
25. Wang, H. P., and Yates, J. T., Jr., *J. Catal.* **89,** 79 (1984).
26. Pearce, H. A., and Sheppard, N., *Appl. Surf. Sci.* **59,** 205 (1976).
27. Coenen, J. W. E., and Linsen, R. G., *in* "Physical and Chemical Aspects of Adsorbents" (B. G. Linsen, Ed.), p. 471. Academic Press, New York/London, 1979.
28. Coenen, J. W. E., *in* "Preparation of Catalysts II" (P. Grange, P. A., Jacobs, and G. Poncelet, Eds.), p. 89. Elsevier, The Netherlands, 1979.
29. Primet, M., and Sheppard, N., *J. Catal.* **41,** 258 (1976).
30. Galuzska, J., and Amenomiya, Y., *in* "Catalysis on the Energy Scene" (S. Kaliaguine and A. Mahay, Eds.), p. 163. Elsevier, The Netherlands, 1984.
31. Hollins, D., Davies, K. J., and Pritchard, J., *Surf. Sci.* **138,** 75 (1984).
32. Hammaker, R. M., Francis, S. A., and Eischens, R. P., *Spectrochim. Acta* **21,** 1295 (1965).
33. Crossley, A., and King, D. A., *Surf. Sci.* **68,** 528 (1977).

34. Campuzano, J. C., and Greenler, R. G., *Surf. Sci.* **83,** 301 (1979).
35. Christmann, K., Shober, O., and Ertl, G., *J. Chem. Phys.* **60,** 4719 (1974).
36. Doyen, G., and Ertl, G., *Surf. Sci.* **43,** 197 (1974).
37. Mitchell, G. E., Gland, J. L., and White, J. M., *Surf. Sci.* **131,** 167 (1983).
38. White, J. M., *J. Phys. Chem.* **87,** 915 (1983).
39. Goodman, D. W., Yates, J. T., Jr., and Madey, T. E., *Surf. Sci.* **93,** L135 (1980).
40. Stoop, F., Toolenaar, F. J. C. M., and Ponec, V., *J. Catal.* **73,** 50 (1982).
41. Dalmon, J. A., and Martin, G. A., *in* "New Horizons in Catalysis" (T. Sciyama and K. Tanabe, Eds.), p. 402. Elsevier, The Netherlands, 1981.
42. Blackmond, D. G., and Ko, E. I., unpublished results.
43. Hicks, R. F., Yen, Q.-J., and Bell, A. T., *J. Catal.* **89,** 498 (1984).
44. Hicks, R. F., and Bell, A. T., *J. Catal.* **90,** 205 (1984).
45. Palazov, A., Kadinov, G., Bonev, Ch., and Shopov, V., *Commun. Chem. Bulg. Acad. Sci.* **11,** 785 (1978).
46. Palazov, A., Kadinov, G., Bonev, Ch., and Shopov, V., *J. Catal.* **74,** 44 (1982).